(12) INTERNATIONAL APPLICATION PUBLISHED UNDER THE PATENT COOPERATION TREATY (PCT)

(19) World Intellectual Property Organization
International Bureau

(43) International Publication Date
29 December 2005 (29.12.2005)

PCT

(10) International Publication Number
WO 2005/124908 A2

(51) International Patent Classification[7]: H01M 8/00

(21) International Application Number:
PCT/US2005/021220

(22) International Filing Date: 14 June 2005 (14.06.2005)

(25) Filing Language: English

(26) Publication Language: English

(30) Priority Data:
60/579,447 14 June 2004 (14.06.2004) US

(71) Applicant *(for all designated States except US)*: **BALLARD POWER SYSTEMS INC.** [CA/CA]; 4343 North Fraser Way, Burnaby, British Columbia V5J 5J9 (CA).

(71) Applicant *(for ZW only)*: **BALLARD POWER SYSTEMS CORPORATION** [US/US]; 15001 Commerce Drive North, Dearborn, MI 48120 (US).

(72) Inventors; and

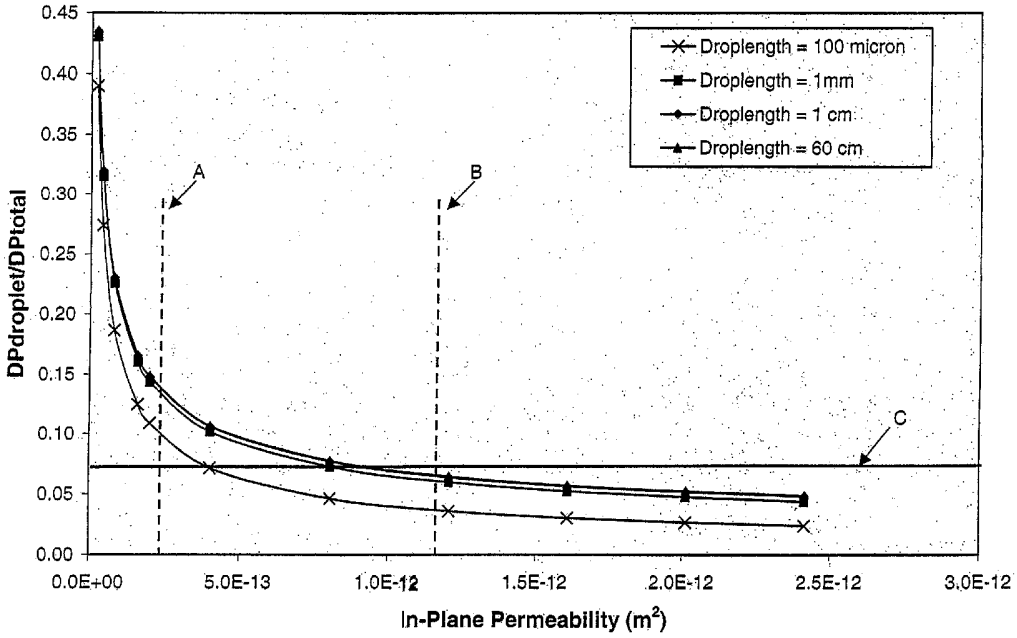
(75) Inventors/Applicants *(for US only)*: **HAAS, Herwig, R.** [DE/CA]; #130-2050 Scotia Street, Vanvouver, British Columbia V5T 4T1 (CA). **CHENG, Derek, Chi Lok** [CA/CA]; 4003 Parker Street, Burnaby, British Columbia V5C 3B8 (CA). **FONG, Kelvin, Keen-Ven** [CA/CA]; 1505 Willingdon Avenue, Burnaby, British Columbia V5C 5H8 (CA). **GLANDT, Jeffrey, D.** [US/CA]; #102-3707 Cambie Street, Vancouver, British Columbia V5Z 2X4 (CA). **LIM, Chuey-Yeng** [MY/CA]; 3953 Godwin Avenue, Burnaby, British Columbia V5G 4A1 (CA). **STARTEK, Cara, N.** [CA/CA]; #4-1312 East 8th Avenue, Vancouver, British Columbia V5N 1T2 (CA).

(74) Agents: **HERMANNS, Karl, R.** et al.; Seed Intellectual Property Law Group PLLC, Suite 6300, 701 Fifth Avenue, Seattle, WA 98104-7092 (US).

(81) Designated States *(unless otherwise indicated, for every kind of national protection available)*: AE, AG, AL, AM, AT, AU, AZ, BA, BB, BG, BR, BW, BY, BZ, CA, CH, CN, CO, CR, CU, CZ, DE, DK, DM, DZ, EC, EE, EG, ES, FI, GB, GD, GE, GH, GM, HR, HU, ID, IL, IN, IS, JP, KE, KG, KM, KP, KR, KZ, LC, LK, LR, LS, LT, LU, LV, MA, MD, MG, MK, MN, MW, MX, MZ, NA, NG, NI, NO, NZ, OM, PG, PH, PL, PT, RO, RU, SC, SD, SE, SG, SK, SL, SM, SY, TJ, TM, TN, TR, TT, TZ, UA, UG, US, UZ, VC, VN, YU, ZA, ZM, ZW.

[Continued on next page]

(54) Title: FLUID DIFFUSION LAYERS WITH IN-PLANE PERMEABILITY CHARACTERISTICS FOR IMPROVED PERFORMANCE IN FUEL CELLS



(57) Abstract: Water management in solid polymer electrolyte fuel cells may be affected by the in-plane permeability characteristics of component fluid diffusion layers. In solid polymer electrolyte fuel cell stacks, performance can be improved by employing fluid diffusion layers in the stack that all have acceptably low in-plane permeability.

WO 2005/124908 A2

(84) Designated States *(unless otherwise indicated, for every kind of regional protection available)*: ARIPO (BW, GH, GM, KE, LS, MW, MZ, NA, SD, SL, SZ, TZ, UG, ZM, ZW), Eurasian (AM, AZ, BY, KG, KZ, MD, RU, TJ, TM), European (AT, BE, BG, CH, CY, CZ, DE, DK, EE, ES, FI, FR, GB, GR, HU, IE, IS, IT, LT, LU, MC, NL, PL, PT, RO, SE, SI, SK, TR), OAPI (BF, BJ, CF, CG, CI, CM, GA, GN, GQ, GW, ML, MR, NE, SN, TD, TG).

Published:

— *without international search report and to be republished upon receipt of that report*

For two-letter codes and other abbreviations, refer to the "Guidance Notes on Codes and Abbreviations" appearing at the beginning of each regular issue of the PCT Gazette.

FLUID DIFFUSION LAYERS WITH IN-PLANE PERMEABILITY CHARACTERISTICS FOR IMPROVED PERFORMANCE IN FUEL CELLS

BACKGROUND OF THE INVENTION

Field of the Invention

The invention relates to fluid diffusion layers having in-plane permeability characteristics that can provide for improved fuel cell performance. In particular, it relates to gas diffusion layers for solid polymer electrolyte fuel cell stacks.

Description of the Prior Art

Fuel cell systems are presently being developed for use as power supplies in a wide variety of applications, such as stationary power plants and portable power units. Such systems offer the promise of efficiently and economically delivering power while providing environmental benefits.

Fuel cells convert fuel and oxidant reactants to generate electric power and reaction products. They generally employ an electrolyte disposed between cathode and anode electrodes. A catalyst typically induces the desired electrochemical reactions at the electrodes.

A preferred fuel cell type, particularly for portable and motive applications, is the solid polymer electrolyte (SPE) fuel cell which comprises a solid polymer electrolyte and operates at relatively low temperatures.

SPE fuel cells commonly employ a planar membrane electrode assembly (MEA) comprising the solid polymer electrolyte or ion-exchange membrane disposed between the cathode and anode. Each electrode contains a catalyst layer, comprising an appropriate catalyst, located next to the solid polymer electrolyte. The catalyst is typically a precious metal composition (*e.g.*, platinum metal black or an alloy thereof) and may be provided on a suitable support (*e.g.*, fine platinum particles supported on a carbon black support). The catalyst layers may contain ionomer similar to that used for the solid polymer membrane electrolyte (*e.g.*, Nafion®). The electrodes typically also contain, or are adjacent to, a porous, electrically conductive substrate that may be

employed for purposes of mechanical support, electrical conduction, and/or reactant distribution, thus serving as a fluid diffusion layer. Flow field plates with distribution channels or passages for directing the reactants across one surface of each fluid diffusion layer are disposed on each side of the MEA. In operation, the output voltage of an individual fuel cell under load is generally below one volt. Therefore, in order to provide greater output voltage, numerous cells are usually stacked together and are connected in series to create a higher voltage fuel cell series stack.

A broad range of reactants have been contemplated for use in SPE fuel cells and such reactants may be delivered in gaseous or liquid streams. The oxidant may, for example, be substantially pure oxygen or a dilute oxygen stream such as air. The fuel stream may be substantially pure hydrogen gas, a gaseous hydrogen-containing reformate stream derived from a suitable feedstock, or a suitable gaseous or liquid organic fuel mixture. In fuel cells supplied with gaseous reactants, the fluid diffusion layers are known as gas diffusion layers or GDLs.

During normal operation of a SPE fuel cell, fuel is electrochemically oxidized at the anode catalyst, typically resulting in the generation of protons, electrons, and possibly other species depending on the fuel employed. The protons are conducted from the reaction sites at which they are generated, through the electrolyte, to electrochemically react with the oxidant at the cathode catalyst. The electrons travel through an external circuit providing useable power and then react with the protons and oxidant at the cathode catalyst to generate water reaction product.

Most membrane electrolyte materials need to be kept hydrated in order to maintain adequate ionic conductivity. In fuel cells employing gaseous reactants, this is typically accomplished by humidifying one or both of the supplied reactant streams.

An important consideration in the design and operation of SPE fuel cells is the management and/or distribution of the water within. A substantial amount of water by-product may be generated during operation and various non-uniformities exist in the structure and in the reaction conditions within the fuel cell. Consequently, water vapor may condense in certain regions of the fuel cell. This liquid water can cause problems, for instance by impeding access of reactants around the catalysts or by blocking the flow field channels. These channels can however be kept clear of liquid

water blockages by ensuring that a sufficiently high reactant pressure drop exists over the channel, thereby continuously forcing liquids out of the channel. Achieving this though may require relatively high reactant supply pressures and thus relatively high parasitic loads leading to reduced system efficiency.

It is desirable therefore to develop fuel cell constructions that can reliably provide for adequate water management without needing relatively high reactant pressures.

BRIEF SUMMARY OF THE INVENTION

In SPE fuel cells, the permeability of gas diffusion layers in a direction parallel to the plane of the layers has been found to be an important characteristic with respect to water management and cell performance. Herein, this permeability parallel to the plane is referred to as the in-plane permeability (IPP) of the fluid diffusion layer. In order to operate the cell at low reactant supply pressures while still adequately removing liquid water from the flow field channels, the IPP should be less than a certain specific value. The actual value will depend on various factors relating to the design and operation of the fuel cell. The lower the IPP is in the GDL, the greater the force will be on water droplets in an adjacent flow field plate. "Gas shorting" around a blocked channel in the flow field plate would thus be reduced. While planar constructions are perhaps most common for SPE fuel cell stacks, other configurations are possible (*e.g.*, spirally wound or undulate MEA constructions). These other configurations may also be expected to benefit from GDLs with lower IPP.

We have discovered that some common materials used as GDLs may have widely varying IPP characteristics. Further, wide variations in the IPP characteristics may exist after certain coatings or other layers are applied to the base materials making up the GDLs. In fuel cell stacks comprising many individual fuel cells, a cell comprising a GDL with unacceptably high IPP may result in corresponding unacceptable cell performance and this in turn may ultimately lead to failure of the entire stack. Thus, it is advantageous for the IPP to be reproducibly low in all the GDLs of a fuel cell stack. Still further, calculation suggests that employing GDLs with even lower IPP than is currently in use, can provide for more reliable stack performance

and/or operation at lower and hence more efficient reactant supply pressures. (That is, being able to reduce the pressure of a compressed air supply can significantly reduce parasitic power losses and improve system efficiency.) However, it is important to maintain a suitably high through-plane gas diffusivity (*i.e.*, normal to the plane of the GDL) such that reactants and by-products can still move easily between the catalyst layers and the flow field plates. (With regard to the transport of reactant and by-products through the GDL which are driven by concentration gradients, the through-plane diffusivity characteristics are more important than the through-plane permeability characteristics.)

A method for quantifying IPP in a GDL is to employ a Gurley device which non-destructively measures the time it takes for a known volume of air under a known driving force to permeate laterally through the GDL. The Gurley time is thus inversely proportional to IPP, and generally greater than 20 Gurley seconds. In certain practical embodiments, IPP values of 50 seconds or more are desirable. As mentioned, a certain through-plane diffusivity must still be maintained.

Alternatively, a permeance tester such as a PMI Automated Perm Porometer may be used to determine IPP. This device measures the radial air flow through a sample with a fixed pressure drop applied across the sample. In certain practical embodiments, a nominal IPP value for the GDLs in a stack may be about 30 cc/minute or less, with the upper limit for IPP being a maximum of 70 cc/minute.

GDLs with such characteristics may be prepared by modifying conventional substrate materials such as carbon fiber papers. Alternatively, such GDLs may be made from perforated sheets or meshes that are filled with an appropriate filler. Since permeability is a stronger function of pore radius than diffusivity is, a greater number of smaller pores might desirably be engineered into a GDL such that IPP is reduced IPP without greatly affecting through-plane diffusivity.

In the case of conventional lightweight carbon fiber papers, the IPP typically needs to be reduced substantially. This may be accomplished by applying coatings or layers of a suitable ink that penetrates the substrate, leaving behind solids within the substrate upon drying. A suitable ink for this purpose comprises a carbon powder and a binder, such as polytetrafluoroethylene, in an aqueous suspension.

Preferably, the ink is prepared under high shear such that the agglomerate size and viscosity is reduced, thus allowing the ink to penetrate into the substrate further. High shear can be provided by a mixer whose maximum shearing tip speed is at least 15 m/sec. The use of lower solids content in the ink and compacting the coating after applying also assists penetration. Such a coating may be effective if applied to either side of the substrate. Multiple coatings may be employed as required in order to reduce IPP. Also, additional coatings may be employed for other purposes (*e.g.*, for purposes of reducing roughness or improving adhesion to adjacent catalyst layers).

In addition, methods are also disclosed for manufacturing a solid polymer electrolyte fuel cell incorporating fluid diffusion layers having the selected IPP characteristics, and thus yielding fuel cells having improved performance.

BRIEF DESCRIPTION OF THE DRAWINGS

Figure 1 shows an exploded schematic diagram of a solid polymer electrolyte fuel cell.

Figure 2a shows the cell voltages versus in-plane permeability grouping for stack 1 in Example 2.

Figure 2b shows the fraction of "low voltage" cells as a function of in-plane permeability grouping for both stacks 1 and 2 in Example 2.

Figure 3 compares the anode flow field flow resistances of the two 10 cell stacks of Example 3 with high and low IPP anode GDLs.

Figure 4 shows the calculated relative pressure drop on a water droplet in a flow field channel versus the in-plane permeability of the adjacent gas diffusion layer in the model fuel cell of Example 4.

Figure 5 shows the average in-plane permeability of Example anodes at various stages of processing into a MEA.

DETAILED DESCRIPTION OF THE INVENTION

An exploded schematic view of a single solid polymer electrolyte fuel cell is depicted in Figure 1. Cell 1 comprises solid polymer electrolyte membrane electrolyte 2, gas diffusion cathode 3, and gas diffusion anode 4. Cathode 3 comprises

gas diffusion layer 5 and catalyst layer 6. In a like manner, anode 4 comprises gas diffusion layer 7 and catalyst layer 8. Adjacent the gas diffusion layers 5, 7 are cathode flow field plate 9 and anode flow field plate 10. Each plate comprises flow field channels to carry reactants and by-product water. Figure 1 shows anode flow field channels 11 in which the direction of the fuel reactant provided is indicated by arrows 12.

The various layers making up the electrodes in Figure 1 are all porous and thus permeable to some degree. The three permeability directions in anode gas diffusion layer 7 are indicated by X, Y, Z axes 13. The in-plane permeability or IPP directions in layer 7 are indicated by axes X and Y. Axis Z represents the through-plane direction. In principle, a water blockage in an anode flow field channel 12 can be bypassed if gas in channel 12 instead travels through gas diffusion layer 7 in the X direction. A water blockage can also cause gas from one channel to travel through gas diffusion layer 7 in the Y direction to an adjacent channel.

As exemplified below, we have discovered that IPP is an important consideration in the design and operation of SPE fuel cell stacks. In particular, stacks operating at low reactant supply pressures or stoichiometries may be more sensitive to the IPP of the component GDLs. (Herein, stoichiometry refers to the ratio of reactant supplied to that consumed in the electricity generating reactions taking place within the fuel cell stack.) As shown in the Examples below, high IPP values in anode GDLs of certain fuel cell stacks have been associated with low cell voltages.

Without being bound by theory, it is believed that marginal conditions for water removal can exist within cells if they comprise GDLs with high in-plane permeabilities and if the cells are provided with reactants at relatively low pressures or stoichiometries. (In the latter case of low stoichiometries, since reactant is consumed as it travels through a flow field, little reactant and hence little reactant pressure may remain near the end of its travel.) In either case, the fluid in the flow field channels may only marginally be able to blow clear any water blockages that form therein. Thus, if any significant amount of fluid bypasses the blockage or is lost to a neighboring channel through the GDL (due to high IPP of the GDL), the water blockage may not be cleared. Over time, the water blockage can then increase in size. Fluid flow to the cell

may be reduced and the region downstream of the blockage becomes reactant depleted. Further, exhaust from other channels or cells may flow back into this region downstream of the blockage. A reactant starvation condition then exists resulting in a low voltage, poorly performing cell. However, it is desirable to operate at conditions of relatively low reactant pressure and stoichiometry for reasons of system efficiency. In order to obtain these system efficiency benefits then, while still avoiding possible water blockages, it is thus desirable to employ GDLs with low IPP.

The choice of an appropriate upper limit for the IPP of GDLs in a given stack will depend on various factors in the stack design and operation. Generally, the IPP of a GDL should be such that pressure sufficient to blow out water droplets would always exist in neighboring flow field channels. This IPP will be a function of GDL geometries (*e.g.*, thickness), flow field geometries (*e.g.*, landing dimensions, channel dimensions), and reactant characteristics (*e.g.*, flow resistances, flow rates, viscosities, pressures). For instance, Example 4 below discusses one method for calculating the relationship between pressure drop across a water droplet and IPP of an adjacent GDL and, from that, deriving a desirable IPP.

Various methods may be used to measure the IPP of a GDL. In the Examples below, IPP was measured using two different methods, the first based on use of a Gurley densometer and the second a permeance tester. These methods are described in more detail below. In an exemplary SPE fuel cell stack suited for powering an automobile, the GDLs might desirably have IPP values greater than about 50 Gurley seconds (as measured using the Gurley densometer). Alternatively, the IPP values for all GDLs in the stack might desirably be less than 70 cc/minute. (Allowing for variation within a typical GDL batch in this case, a nominal IPP value for such GDLs might then be about 30 cc/minute.)

The desired low IPP characteristics may be obtained in GDLs made from fine meshes or finely perforated sheets that have been filled with a suitable porous filler of conductive powder. The impermeable portions of mesh or sheet material can serve to block in-plane permeance. However, other materials might be preferred for reasons of cost, conduction, ease of manufacture, etc. Lightweight carbon fiber paper is presently a preferred GDL material but the IPP of such paper may be undesirably high

and variable. The IPP of carbon fiber paper can be modified successfully though by impregnating it with filler inks, applied in one or more coating steps. In this way, low IPP characteristics can be reliably obtained.

Suitable filler inks comprise carbon powder and binder (*e.g.*, polytetrafluoroethylene) and an optional pore former (*e.g.*, methycellulose) in an aqueous suspension. High shearing rates are preferably used to prepare such inks in order to reduce ink viscosity. High shear can be obtained using mixers with shearing tip speeds over 15 m/sec. Penetration of the paper is also improved when lower solids content is used in the ink and by compacting the coating after applying it. Such impregnating coatings can be effective if applied to either side of the paper. More than one impregnating coating may be employed in order to reduce IPP to the desired level. (A certain through-plane diffusivity must still be maintained, of course.) Also, additional coatings may be employed for other purposes (*e.g.*, to reduce roughness or improve adhesion to adjacent catalyst layers).

Examples

The following Examples are provided to illustrate certain aspects and embodiments of the invention but should not be construed as limiting in any way.

In these Examples, IPP has been measured using two different methods: permeance and Gurley. IPP is proportional to permeance and inversely proportional to Gurley. The former method is more accurate than the latter. However the former method requires a specific sample size and is a more time consuming test.

The permeance method employed a PMI Automated Perm porometer to measure radial air flow through a 4 cm diameter circular sample. A pressure drop of 5 psi across the sample was used each time and measurement time per sample was of order of 10 minutes.

The Gurley method employed a conventional Manual Gurley 4118 densometer (by Gurley Precision Instrument). In-plane permeability was measured by inserting a sample between two plates. The upper plate had a 0.1 sq. in. opening that channelled air through the sample, while the bottom plate had no opening, thus forcing the air in-plane. In all cases, a 25 ml volume of air and a 20 oz cylinder (to apply

pressure) was used. The measurement time per sample here is only of order of 15 seconds.

Example 1

Over a period of months, several SPE fuel cell stacks that employed four slightly different MEA designs were fabricated for automotive use. After operating these stacks for some time at fuel stoichiometries of about 1.15, the voltage outputs of certain cells in the stacks were observed to be significantly lower than the rest of the cells in the stacks. ("Low voltage" was taken to be < 0.7 V under the standard operating conditions.) The number of these "low voltage" cells varied from stack to stack and the location of the "low voltage" cells in the stacks appeared to be random. One of the stacks was then disassembled and the physical properties (including in-plane permeability) of MEAs from a few "low voltage" cells were obtained and compared to MEAs from a few cells showing normal voltages. No statistically significant difference in the physical properties was found between these sets of MEAs, although the sample size tested was relatively small. However, the anode IPP generally was observed to vary significantly, from about 60 to 240 cc/min (as determined by porometer).

The anode IPP characteristics of the MEAs employed over this time period were then compiled and compared to the frequency of occurrence of "low voltage" cells in the fabricated stacks. A significant variation in anode IPP was observed for each MEA design and almost an order of magnitude variability in anode IPP was observed between the four different MEA designs (about 60 to 600 cc/min as determined by porometer). It was noted that the trend of anode IPP appeared to follow that of the occurrence of "low voltage" cells, *i.e.*, over the period of months, stacks made with MEAs having higher anode IPP appeared to show a higher incidence of "low voltage" cells. In particular, in one interval over this time period, "low voltage" cells were not seen. In this interval, a substantial drop in the measured anode IPP had taken place. Further, this drop in anode IPP and the temporary disappearance of "low voltage" cells appeared to coincide with a change in the manufacture of the anodes (*i.e.*, a change in the application of a carbon sublayer).

This example suggested that the incidence of low voltage cells may relate to relatively high anode IPP.

Example 2

A 450 cell SPE fuel cell stack manufactured for use as a bus engine was operated for some time at a fuel stoichiometry of 1.2. After this, approximately 35% of the cells (160) exhibited "low voltages". The stack was disassembled and the anode IPP of each MEA was measured using the Gurley device. (The Gurley device was used because the MEAs needed to be measured non-destructively and in a short time frame. Separate trials have demonstrated a strong correlation between IPP as determined by the porometer and by the Gurley device.)

The 160 MEAs from the "low voltage" cells and a selection of 280 MEAs from the remaining normal cells were then sorted on the basis of anode IPP (in Gurley seconds or Gs) into five categories as shown in the Table below.

Group	12 Gs	14 Gs	18 Gs	22 Gs	24 Gs
Range (in Gs)	IPP<12	12<IPP<16	16<IPP<20	20<IPP<24	24<IPP

A fuel cell stack was then assembled with cells comprising these reclaimed, sorted MEAs. This stack, denoted stack 1, was assembled according to a design for automotive use. The MEAs were arranged so that any differences between the lowest IPP MEAs (24 Gs) and highest IPP MEAs (12 Gs) could be investigated in the same cell row. New separator/flow field plates were also employed in the stack. The coolant channel pressure drop was accurately measured in 220 of these plates and these measured plates were sorted into five groups according to coolant pressure drop. (The remaining plates were not measured.) The plate arrangement in the stack was set up to investigate any interaction of hotter cathodes (assumed to be adjacent plates with higher pressure drop and hence lower coolant flow rate) with colder anodes (assumed to be adjacent plates with lower pressure drop and hence higher coolant flow rate). In this designed experiment, the MEAs and plates were strategically assembled to investigate the effect of the two parameters, IPP and coolant pressure drop.

Stack 1 was then operated for some time at a fuel stoichiometry of 1.15 and the incidence of "low voltage" cells was recorded. Figure 2a shows the relationship between IPP grouping and cell voltage. As seen in Figure 2a, a large number of cells with higher IPP MEAs (12 and 14 Gurley-seconds) exhibited "low voltages", whereas no cells with lower IPP MEAs (*i.e.*, 22 and 24 Gurley-seconds) did. And, a few cells made with MEAs of intermediate IPP (18 Gurley-seconds) exhibited "low voltages". These results clearly show the correlation between IPP and the incidence of "low voltage" cells. The coolant pressure drop in the plates did not however appear to be a significant variable with regards to the incidence of "low voltage" cells.

Stack 1 was then disassembled and the component MEAs were again reclaimed from the cells inside. Another stack, denoted stack 2, was then made using these reclaimed, sorted MEAs in the cells. Stack 2 was assembled according to a design intended for use in a bus. Different separator/flow field plates than those used in stack 1 were employed.

Stack 2 was then operated for some time at a fuel stoichiometry of 1.2 and the incidence of "low voltage" cells was recorded. Similar results to those of stack 1 were obtained, namely a correlation between higher IPP and the incidence of "low voltage" cells. Figure 2b shows the fraction of "low voltage" cells in the stack as a function of IPP grouping. (The filled and unfilled bars denote stack 1 and stack 2 respectively.)

The designed experiments of this example show a clear correlation between IPP and cell performance.

Example 3

Two 10 cell SPE fuel cell stacks (A and B) were assembled in which stack A comprised anode GDLs having high in-plane permeabilities and stack B comprised similar anode GDLs but having low in-plane permeabilities. (The B stack GDLs had IPP values in the range from about 1300 to 1550 Gurley seconds. The A stack GDLs ranged from 250 to 650 Gurley seconds with one exception at about 2000 Gurley seconds.)

A set of trials was then performed in which the flow resistances of the anode flow fields were measured after operating the stacks. Each stack was run and measured three times in their wet state. The order the stacks were run was selected randomly however. In each case, the stacks were run at low fuel stoichiometry (1.2), low load conditions for an hour. Flow resistance values were obtained for all the anode flow fields except those in the end cells of the stacks. In order to make these measurements, the stacks were disassembled (but without disturbing the membrane/anode GDL/anode flow field interfaces) and each flow field was measured individually. The stacks were then reassembled in the same order and run again. Finally, the stacks were dried and the dry flow resistances were measured as well.

The results are shown in the bar chart of Figure 3. As the stack trial sequence turned out to be B A A B B A, the results for each cell appear in this order too (*i.e.*, from left to right, the order is: B stack trial 1, A stack trial 1, A stack trial 2, etc.). The last two bars associated with each cell represent the dry flow resistances in the B and A stacks (the next-to-last and last bars respectively). As is apparent from Figure 3, the flow resistances observed in the A stack were irregular and often significantly higher than those of the B stack or those of either stack when dry.

This example shows that higher IPP in the anode GDLs is associated with increased flow resistance during operation. This would be consistent with water blockages being present in the high IPP cells.

Example 4

Because the poor cell performance associated with anode IPP is believed to stem from water blockages in the associated flow field channels, an attempt was made to model this phenomena. A single cell intended for use in an automotive application was assumed. In this single cell model, the flow field was taken to be a high aspect ratio design (length much greater than width) comprising multiple parallel flow channels along its length. The force required to move a water droplet along a channel was presumed to come solely from the flow of gas at a certain pressure in that channel. Since the anode GDL is permeable, a portion of the gas flow in that channel was assumed to tunnel around the droplet through the GDL and back into the channel,

thus bypassing the water droplet. The magnitude of the force exerted by the gas flow on the droplet is thus a function of the permeability of the GDL.

In order to initiate movement of the water droplet, a critical force is needed to overcome a combination of frictional, viscous, tension, and capillary forces along the perimeter of the droplet. The critical force is difficult to calculate accurately but can be measured empirically. For a fixed channel geometry (*e.g.*, fixed cross-section), a critical pressure drop is needed to move the water droplet.

A simple network model was created to study the impact of IPP on the pressure drop expected across a water droplet blocking a channel. This network model attempted to model in a simplistic way the flow tunneling around a droplet and also through the GDL to neighbouring channels. Darcy's Law was taken to govern flow and pressure drop in the GDL. The Hagen-Poiseillue equation was taken to govern flow and pressure drop in the channel. Both Darcy's Law and the Hagen-Poiseillue equation can be simplified to a basic resistor type relationship (similar to Ohm's law). Using this resistor relationship, the pressure drops and flows in the cell were modeled as a series of resistors. A network of pressure nodes was set up in which each node was connected to the adjacent node by the flow resistor equation. A single water droplet was assumed to be located in the centre of an intermediate flow channel as an obstruction to gas flow. Using a set of dimensions and operating conditions representative of this automotive type of fuel cell, the network model was solved for pressure drop across the droplet as a function of anode IPP.

Figure 4 shows the results calculated for varied droplet sizes (specifically, droplet length). In Figure 4, the y axis represents the pressure drop across the droplet relative to the total pressure drop across the flow field. The x axis represents permeability in m^2. As shown in Figure 4, the model predicts that as the IPP is decreased to very low values, the pressure drop across the droplet increases very significantly. However, the pressure drop across the droplet does not vary so significantly over higher IPP values. Also, the results show little dependence on droplet lengths above values of 1 mm.

The model illustrates why, in Example 1 above, MEAs with higher IPP might be associated with low voltage cells, while MEAs with lower IPP might not be.

For reference, the IPP range for the anodes of Example 1 (*i.e.*, 60 to 600 cc/min as determined by porometer) is marked by vertical lines A and B. An empirical value of the critical pressure drop required to move a 2.2 mm water droplet along a single channel is also marked by the horizontal line C. (This value was obtained using a "see-through" experimental fuel cell assembly that otherwise duplicated the construction of the fuel cell. The critical pressure was determined visually by observing what pressure was required to move a water droplet within a channel.) For water droplets of this size, the region below line C indicates IPP values where water droplets cannot be removed. If this were a typical size of a water droplet in a channel, it would be expected that droplets would be cleared away in cells made with MEAs from the low permeability end of range A-B and thus these cells should function normally. On the other hand, it would be expected that droplets would not clear from cells made with MEAs from the high permeability end of range A-B and thus these cells should not function as well.

The model also suggests that employing a GDL with very low IPP should allow for a substantial reduction in the total pressure drop across the cell, while still providing a high enough pressure drop across a blocking water droplet to move it along the channel. Hence, employing GDLs with very low IPP could lead to significant savings in parasitic system energy losses

Example 5

In Example 1, a significant variation in anode IPP was seen within each MEA design as well as within the four MEA designs tested (the latter ranged from about 60 to 600 cc/min). A significant variation has also been seen in the IPP of the GDLs themselves and in the IPP of the materials used in making GDLs.

Carbon fiber paper obtained from Toray is frequently used in the art as a GDL substrate. Here, TGPH60 carbon fiber paper from Toray was treated to render it hydrophobic (by impregnating with polytetrafluoroethylene, PTFE, using an aqueous suspension and then sintering the PTFE impregnated paper). The IPP of four samples was measured using the porometer method. The IPP ranged from about 350 to 580 cc/min. A surface layer comprising carbon powder and PTFE binder was then screen printed to one side of the hydrophobic paper. Such surface layers are frequently

employed in the art to provide an appropriate surface upon which catalyst can be coated to form a gas diffusion electrode. The IPP of several samples was measured using the porometer method (with air pressure being applied to the uncoated side of the sample). The IPP ranged from about 70 to 280 cc/min.

This Example shows that conventional materials used for GDLs show significant variation in IPP. Conventional screen printed coatings or sublayers reduce the IPP but a significant variation may still be seen.

Example 6

A designed experiment was performed to study the IPP obtained when two carbon layers were applied to hydrophobic carbon fiber paper similar to that used in Example 5. In this experiment, a first carbon layer was applied with the intent of impregnating the paper and then a second carbon layer was applied afterwards to provide an appropriate surface upon which to coat a catalyst layer. The first carbon layer was applied via a screen printing technique using an aqueous ink (11% solids) comprising 67% carbon powder, 18% PTFE, and 15% methylcellulose (a pore former). For purposes of better penetration into the paper, the ink was mixed in a high shear mixer with a maximum tip speed of 15 m/s in order to reduce agglomerate size and viscosity. The viscosity (as measured by a Brookfield viscometer at 60 rpm, a shear rate of 1/13 s^{-1}) was about 5900 cP. Several different ratios of carbon powder (varying from 64 to 86%), PTFE (varying from 6 to 21%) and methylcellulose (varying from 8 to 15%) were used in inks for the second carbon layer. In each case, the ink comprised 5% solids and was mixed in a high shear mixer with a maximum tip speed of 17 m/s. Viscosities ranged from 40 to 280 cP. The second layer was applied in a similar manner using a screen printing process. The total carbon loading (both coats) was 2 mg/cm^2.

A matrix of 30 different anode gas diffusion layers, GDLs, were prepared in this way. A catalyst layer was applied in a conventional manner to each GDL followed by an ionomer spray coating to form a gas diffusion electrode, GDE. An elastomeric perimeter seal was then applied to each GDE (for purposes of sealing in an

assembled fuel cell). Finally each perimeter sealed GDE was assembled into a complete membrane electrode assembly, MEA.

At various stages in the preceding, the IPP of representative samples were measured in multiple locations using the permeance method. Figure 5 shows the average IPP of the samples (all measurements were included in these averages) at these various stages of preparation, namely the hydrophobic carbon fiber paper alone (denoted HCFP), after first carbon layer applied (denoted C1), after second carbon layer applied (denoted C2), after Pt catalyst layer applied (denoted Pt), and finally the complete membrane electrode assembly (denoted MEA). About a five fold reduction in IPP was obtained with the application of the first layer. A further reduction from about 96 to 68 cc/min occurred with application of the second layer (indicating that a certain level of penetration occurs with the second layer). The IPP reduction seen with the application of the catalyst layer is believed to result from the sintering of PTFE, where the individual PTFE particles melt and combine to form a web within the GDE.

In all samples, the anode IPP in the MEAs was less than 50 cc/min. The preceding method would therefore appear to be suitable for reliably preparing MEAs with low anode IPP.

While particular elements, embodiments and applications of the present invention have been shown and described, it will be understood that the invention is not limited thereto since modifications may be made by those skilled in the art without departing from the spirit and scope of the present disclosure.

CLAIMS

What is claimed is:

1. A solid polymer electrolyte fuel cell stack comprising a plurality of fuel cells, each fuel cell in the stack comprising a gas diffusion layer associated with an electrode in the cell, and each gas diffusion layer characterized by a through-plane permeability and an in-plane permeability, wherein the in-plane permeability of each gas diffusion layer as measured by Gurley method is greater than 20 Gurley seconds.

2. The fuel cell stack of claim 1 wherein the in-plane permeability of each gas diffusion layer as measured by Gurley method is greater than 50 Gurley seconds.

3. The fuel cell stack of claim 1 wherein the in-plane permeability of each gas diffusion layer as measured by permeance method is less than 70 cc/min.

4. The fuel cell stack of claim 3 wherein the in-plane permeability of each gas diffusion layer as measured by permeance method is less than 30 cc/min.

5. The fuel cell stack of claim 1 wherein the electrode in each cell is the anode.

6. The fuel cell stack of claim 1 wherein the fuel cells in the stack are planar.

7. The fuel cell stack of claim 1 wherein the gas diffusion layers comprise carbon fiber paper.

8. The fuel cell stack of claim 7 wherein the gas diffusion layers consist essentially of carbon fiber paper and filler.

9. The fuel cell stack of claim 8 wherein the filler comprises carbon powder and a binder.

10. The fuel cell stack of claim 9 wherein the binder is polytetrafluoroethylene.

11. The fuel cell stack of claim 1 wherein the gas diffusion layers comprise sheets of expanded graphite.

12. A method of manufacturing a solid polymer electrolyte fuel cell stack, the stack comprising a plurality of fuel cells, each fuel cell in the stack comprising a gas diffusion layer associated with an electrode in the cell, and each gas diffusion layer characterized by a through-plane permeability and an in-plane permeability, the method comprising reducing the in-plane permeability of each gas diffusion layer such that the permeability as measured by Gurley method is greater than 20 Gurley seconds.

13. The method of claim 12 comprising preparing each gas diffusion layer by obtaining a porous substrate and applying a filler to the substrate.

14. The method of claim 13 wherein the substrate is a carbon fiber paper.

15. The method of claim 13 wherein the filler is applied by way of an ink.

16. The method of claim 15 comprising preparing the ink under high shear.

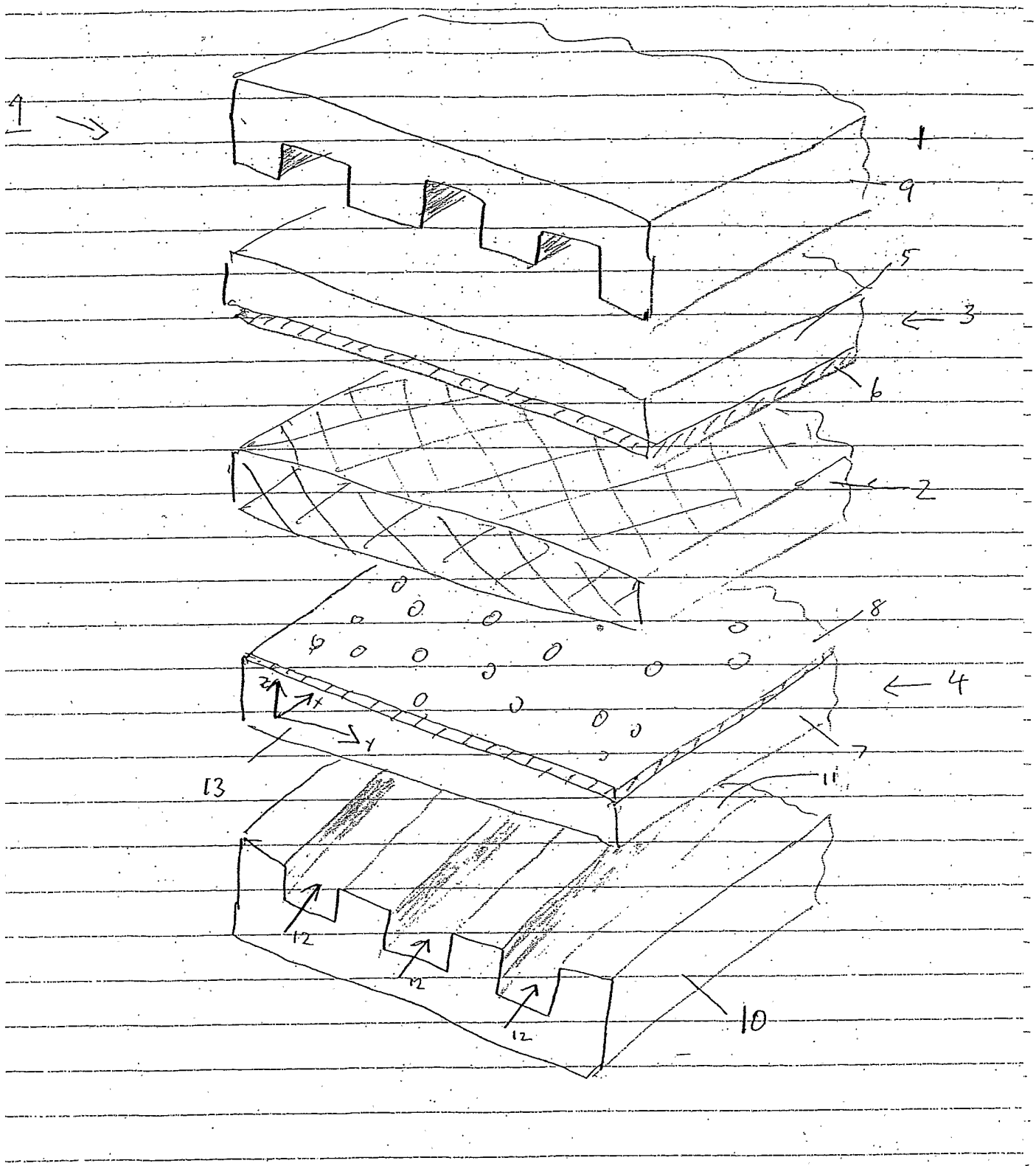


FIGURE 1

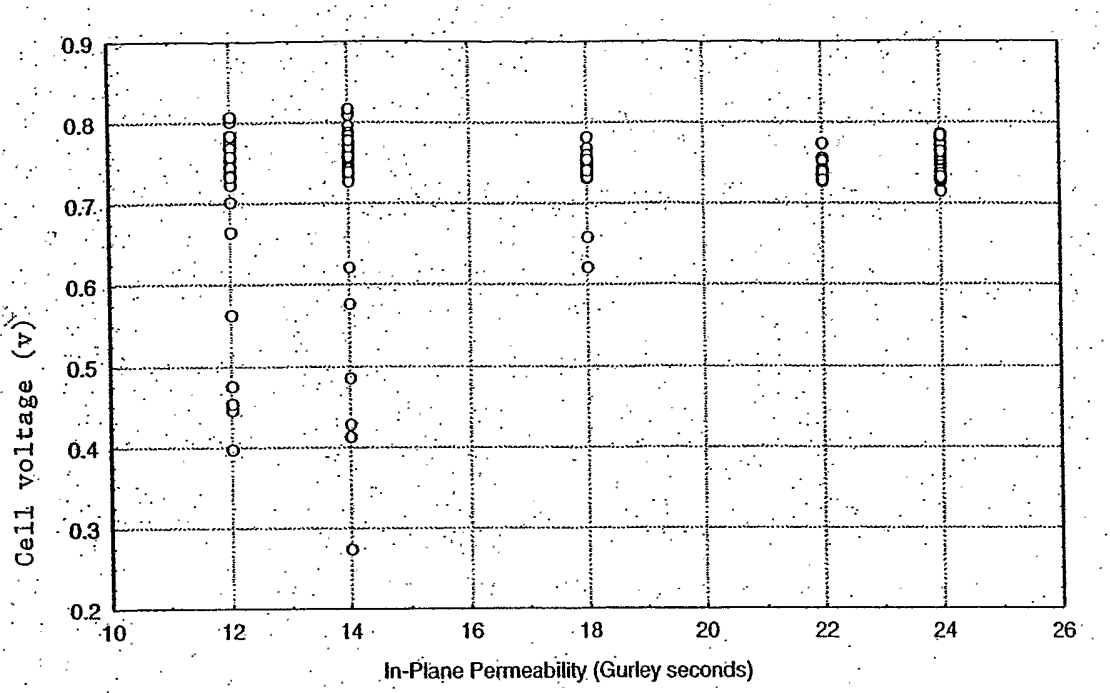

Cell voltage (v)
0.9
0.8
0.7
0.6
0.5
0.4
0.3
0.2
10
12
14
16
18
20
22
24
26
In-Plane Permeability (Gurley seconds)

FIGURE 2a

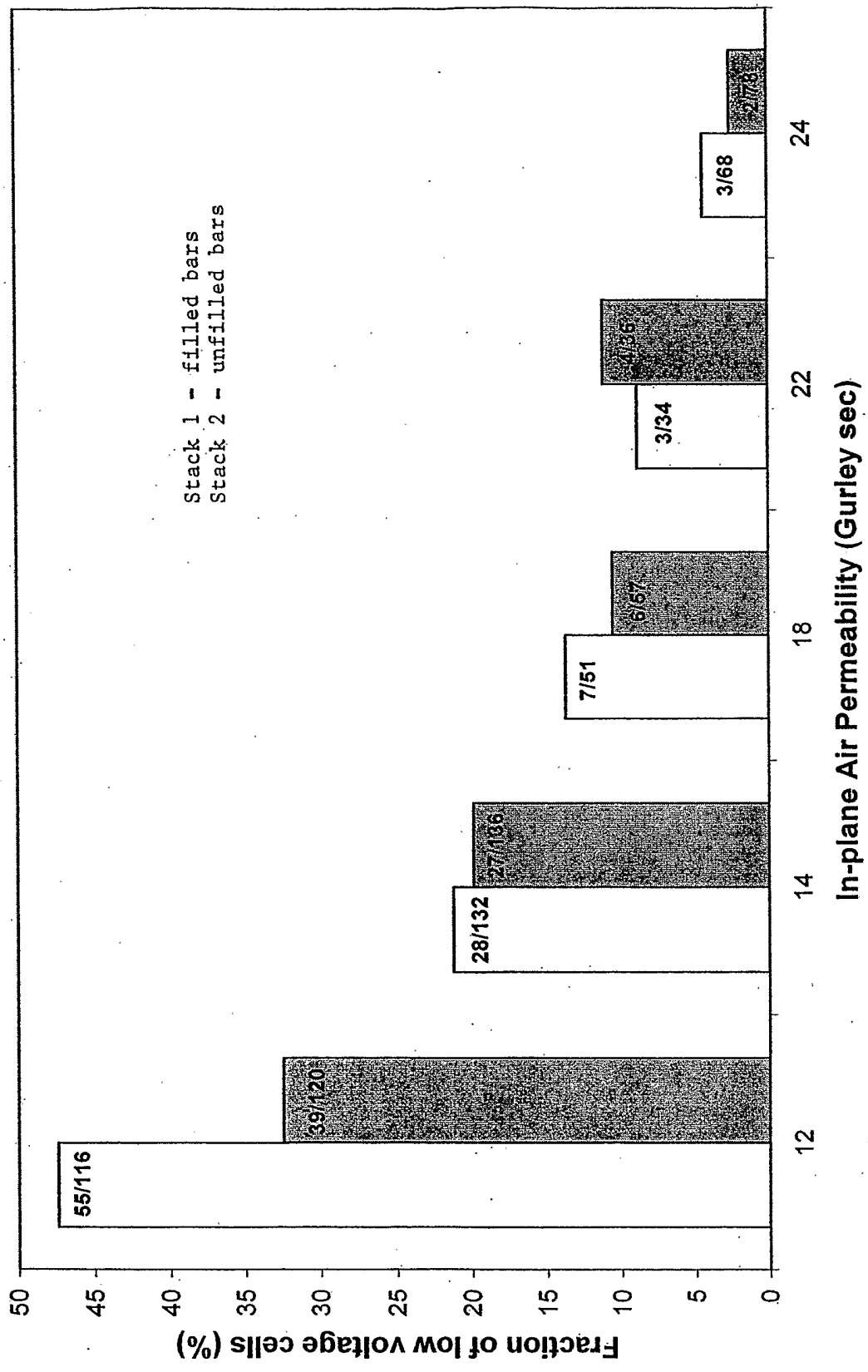

Stack 1 - filled bars
Stack 2 - unfilled bars
55/116
39/120
28/132
27/136
7/51
6/67
3/34
4/36
3/68
2/73
0
5
10
15
20
25
30
35
40
45
50
12
14
18
22
24
Fraction of low voltage cells (%)
In-plane Air Permeability (Gurley sec)

FIG. 2b

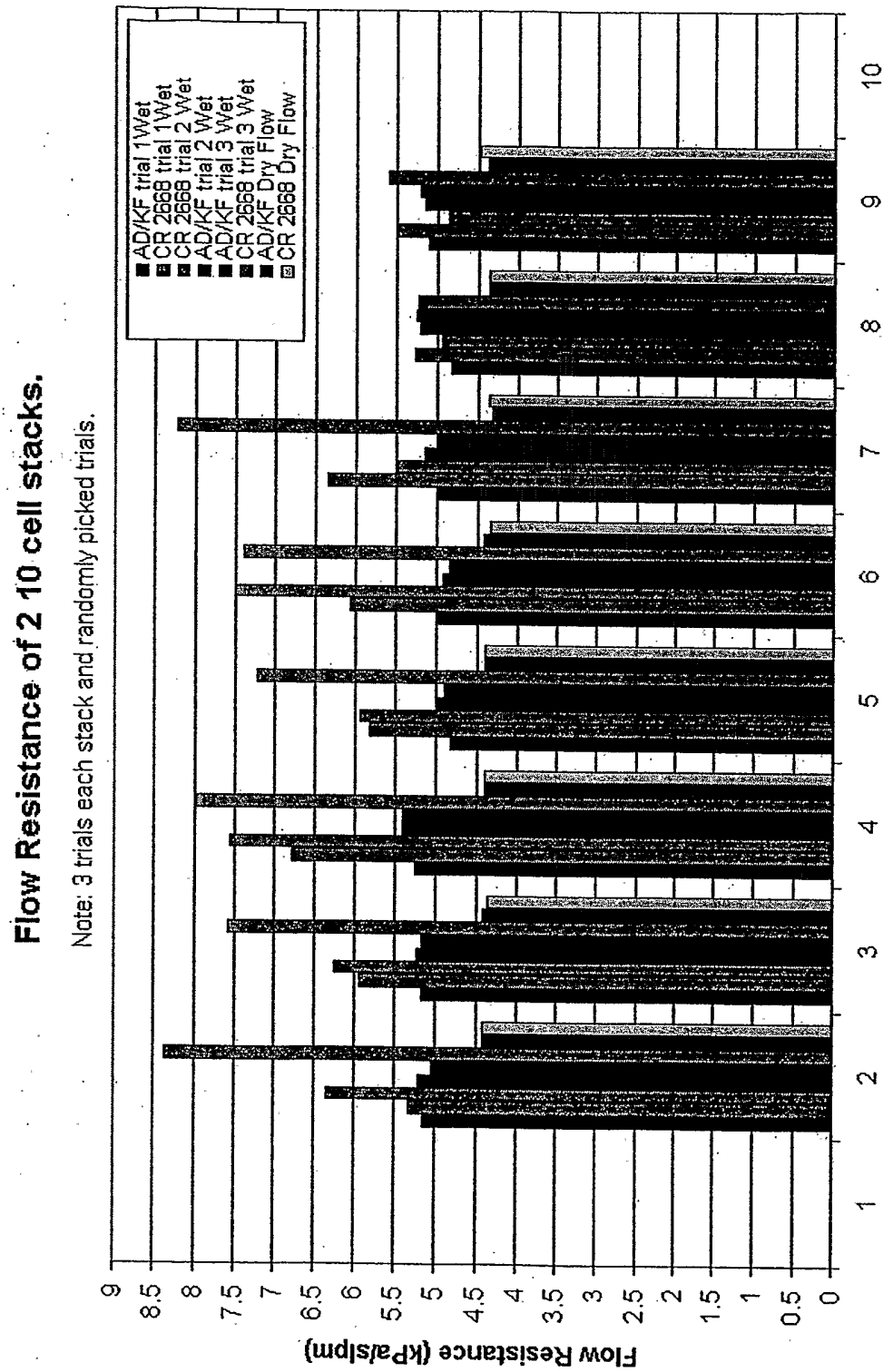

Flow Resistance of 2 10 cell stacks.
Note: 3 trials each stack and randomly picked trials.
AD/KF trial 1Wet
CR 2668 trial 1Wet
CR 2668 trial 2 Wet
AD/KF trial 2 Wet
AD/KF trial 3 Wet
CR 2668 trial 3 Wet
AD/KF Dry Flow
CR 2668 Dry Flow
Flow Resistance (kPa/slpm)
0
0.5
1
1.5
2
2.5
3
3.5
4
4.5
5
5.5
6
6.5
7
7.5
8
8.5
9
1
2
3
4
5
6
7
8
9
10
Cell #

FIGURE 3

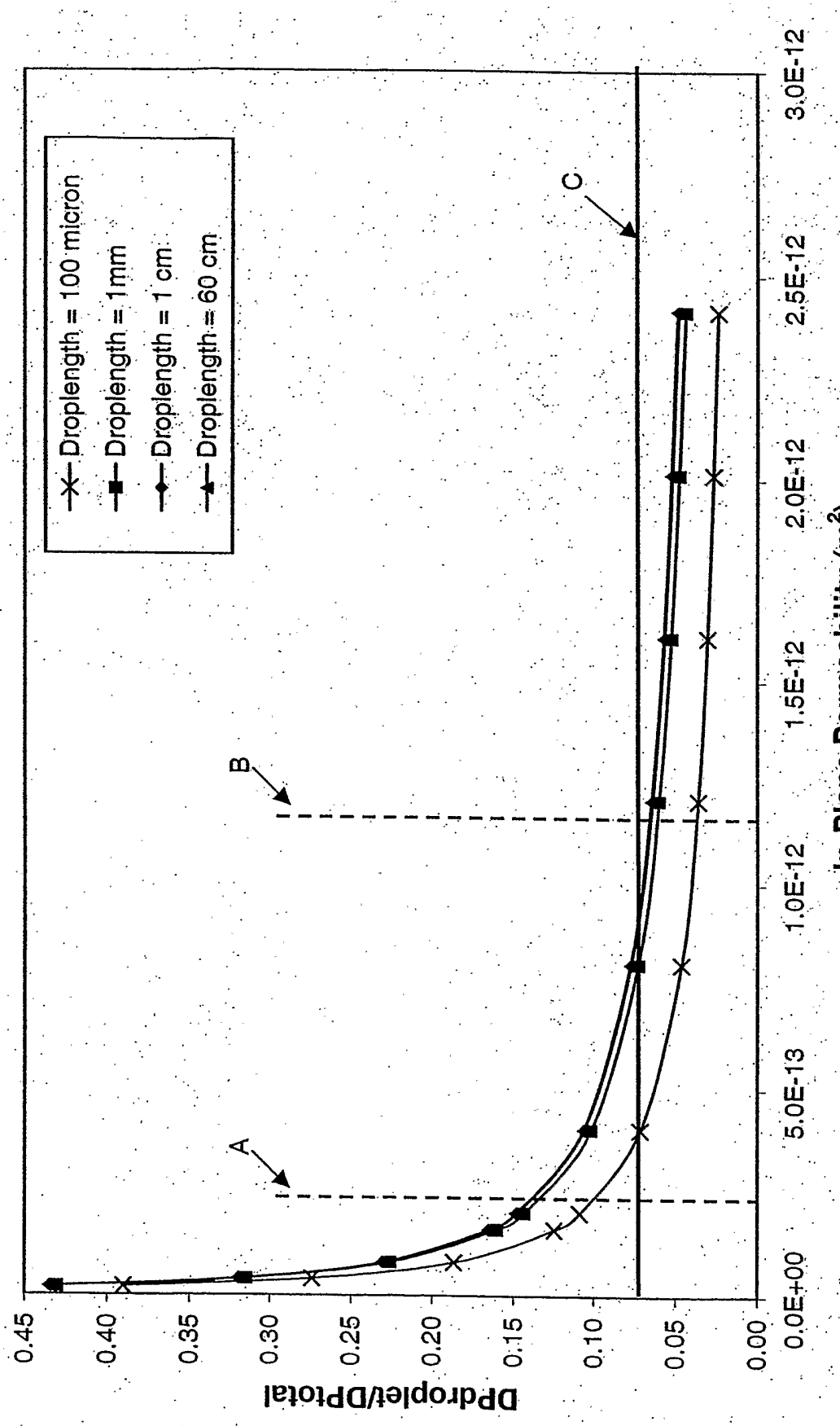

Droplength = 100 micron
Droplength = 1mm
Droplength = 1 cm
Droplength = 60 cm
A
B
C
DPdroplet/DPtotal
0.45
0.40
0.35
0.30
0.25
0.20
0.15
0.10
0.05
0.00
0.0E+00
5.0E-13
1.0E-12
1.5E-12
2.0E-12
2.5E-12
3.0E-12
In-Plane Permeability (m2)

FIG. 4

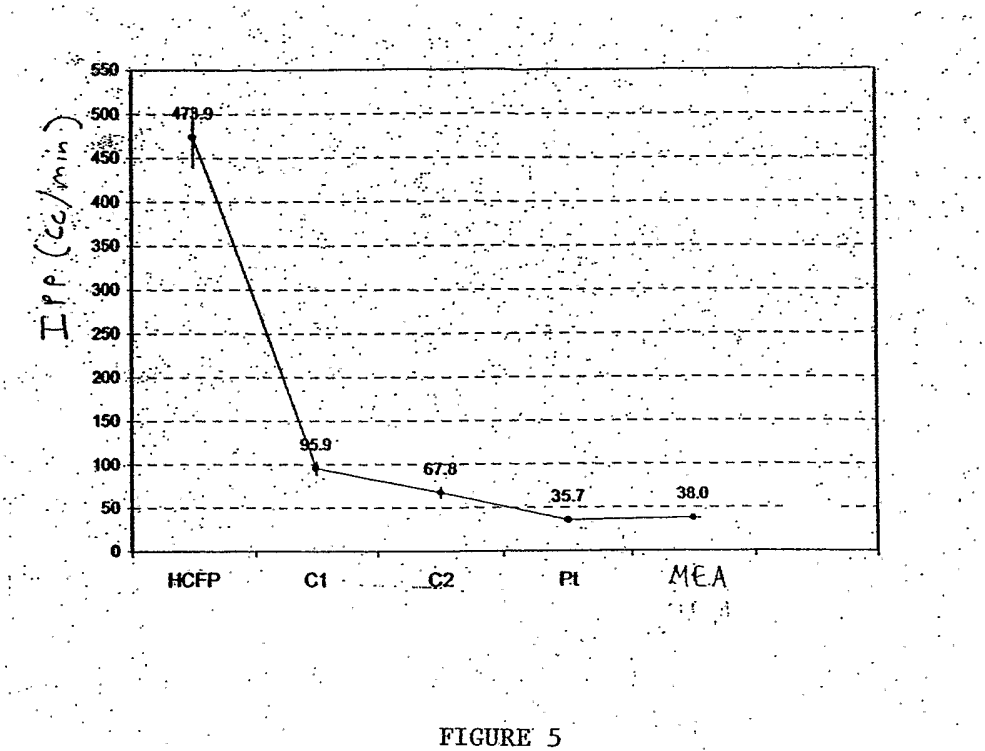

Tpp (cc/min)
550
500
450
400
350
300
250
200
150
100
50
0
473.9
95.9
67.8
35.7
38.0
HCFP
C1
C2
Pt
MEA

FIGURE 5